Portland State University

PDXScholar

Chemistry Faculty Publications and Presentations   Chemistry

8-1-1999

Optical properties of β″-(ET)2SF5CH2CF2SO3: A layered molecular superconductor with large discrete counterions

J. Dong

J. L. Musfeldt

J. A. Schlueter

Jack M. Williams

P. G. Nixon

See next page for additional authors

Let us know how access to this document benefits you.

Follow this and additional works at: http://pdxscholar.library.pdx.edu/chem_fac

Part of the Physics Commons

Citation Details

Dong, J., Musfeldt, J. L., Schlueter, J. A., Williams, J. M., Nixon, P. G., Winter, R. W. and Gard, G. L. (1999). Optical properties of β″-(ET)$_2$SF$_5$CH$_2$CF$_2$SO$_3$: A layered molecular superconductor with large discrete counterions. Physical Review B, 60, 4342.

Authors

J. Dong, J. L. Musfeldt, J. A. Schlueter, Jack M. Williams, P. G. Nixon, Rolf Walter Winter, and Gary L. Gard

Optical properties of β''-$(ET)_2SF_5CH_2CF_2SO_3$: A layered molecular superconductor with large discrete counterions

J. Dong and J. L. Musfeldt

Department of Chemistry, State University of New York at Binghamton, Binghamton, New York 13902-6016

J. A. Schlueter and J. M. Williams

Materials Science Division, Argonne National Laboratory, 9700 South Cass Avenue, Argonne, Illinois 60439

P. G. Nixon, R. W. Winter, and G. L. Gard

Department of Chemistry, Portland State University, Portland, Oregon 97207

(Received 3 March 1999)

We report the polarized infrared and optical reflectance of β''-$(ET)_2SF_5CH_2CF_2SO_3$ as a function of temperature. This fully organic superconductor displays weakly metallic behavior over the entire temperature range of our investigation. The electronic properties present several unusual features including the lack of a conventional free carrier (Drude) response at low temperature, infrared localization phenomena, and an unexpected temperature dependence of the oscillator strength. Similar behavior is observed in other β and β'' superconductors above T_c, suggesting that this class of compounds is very close to a metal $\rightarrow$ insulator transition where electronic correlations are important and the Drude response carries very little spectral weight. Vibronic features increase in intensity with decreasing temperature in the infrared, as expected. The temperature dependence of key anion vibrational modes are discussed in terms of intermolecular hydrogen bonding within the anion pocket. [S0163-1829(99)04330-1]

I. INTRODUCTION

The subject of superconductivity and other competing broken symmetry ground states in ET-based organic conductors [here, ET is bis(ethylenedithio)-tetrathiafulvalene] have received remarkable attention in recent years.[1–3] In this class of materials, the highest superconducting transition temperatures to date are obtained with polymeric counterions in κ-$(ET)_2Cu[N(CN)_2]Br$ ($T_c = 11.6$ K) (Ref. 4) and κ-$(ET)_2Cu[N(CN)_2]Cl$ ($T_c = 12.8$ K at 0.3 kbar).[5] More recently, a strategy for the preparation of ET-based superconductors has been pursued based upon the design of large discrete counterions[6] to enhance two-dimensional interactions in the solid state. The κ-$(ET)_2M(CF_3)_4$(1,1,2-trichloroethane) (Ref. 7) and β''-$(ET)_2SF_5CH_2CF_2SO_3$ (Ref. 8) superconductors are examples of this effort. The strategy of incorporating large, chemically tunable anions is advantageous because it allows the exploration of intermolecular interaction effects on the physical properties. For instance, in the $SF_5RSO_3{}^-$ system, small chemical modifications of the anion template can result in the stabilization of a semiconducting, spin-Peierls, metallic, or superconducting ground state.[9] It is the β''-$(ET)_2SF_5CH_2CF_2SO_3$ superconductor which is of interest here. Much effort has been made to correlate structural features of ET-based conductors with their physical properties,[3] including superconducting transition temperatures. While there are many κ- and β-type superconductors, $(ET)_2SF_5CH_2CF_2SO_3$ ($T_c = 5.2$ K) displays a β'' structure,[8] making it the second example of a β'' superconductor. The only other β'' superconductors are the

$(ET)_4M(ox)_3H_2OC_6H_5CN$ (M = Fe, Cr) salts.[10,11]

The crystal structure of β''-$(ET)_2SF_5CH_2CF_2SO_3$ (inset, Fig. 1) contains conducting ET cation layers alternating with anion layers. The ET molecules form loose stacks along the a axis, although the strongest intermolecular contacts are *between* molecular stacks, which is the b direction.[8] Many short contacts between hydrogen atoms on the ethylene end groups of the ET, and the SF_5 fluorine and SO_3 oxygen atoms on the anion are formed, which act to increase dimensionality and determine counterion ordering within the anion pocket. These short contacts are likely responsible for the β''-packing motif of molecules in the crystal as well as the stabilization of the superconducting ground state. No short
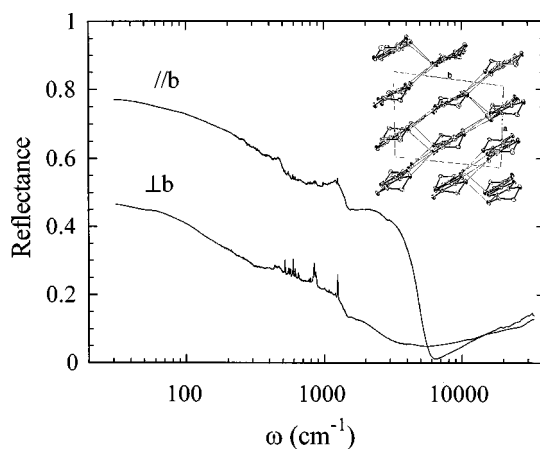

FIG. 1. Polarized infrared and optical reflectance of β''-$(ET)_2SF_5CH_2CF_2SO_3$ at 300 K. The inset displays the crystallographic structure in the ab plane.

contacts are observed between the R group of the anion and the ET molecules for the superconducting salt. It is notable that both the cation and anion are purely organic in this material.

The 300 K dc electrical conductivity of β''-$(ET)_2SF_5CH_2CF_2SO_3$ in the conducting ab plane is weakly metallic (≈ 6 Ω^{-1} cm^{-1}),[12] and much larger than that in the interlayer c direction, in line with what is expected based upon the structure of this compound. The dc conductivity can show two quite different responses as a function of temperature.[12] In some cases, a metallic temperature dependence is observed down to the 5.2 K superconducting transition. In other situations, a maximum is found near 100 K, with metallic temperatures dependence below this point. Cooling rate dependence of anion rearrangements may be responsible for these two behaviors. In both cases, the superconducting transition is sharp, and the in-plane dc conductivity is on the order of 300 Ω^{-1}cm^{-1} near 10 K. The pressure dependence of T_c is typical of that of many ET salts ($dT_c/dP = 1.34$ K/kbar).[13] An estimate of the 300 K microwave conductivity via ESR shows an anisotropy of $\sigma_b/\sigma_a \approx 1.4$ in the conducting plane.[14,15] Analogous to other β'' compounds,[16] electronic band-structure calculations predict a Fermi surface (FS) consisting of a pair of one-dimensional (1D) electronic bands and a two-dimensional (2D) hole pocket, which is 14.8% of the first Brillouin zone (FBZ).[17] More recent calculations suggest that the low-temperature interdimer interaction facilitates the stabilization of superconductivity in β''-$(ET)_2SF_5CH_2CF_2SO_3$.[18] Experimental determination of the FS,[17,19] through magnetic oscillation studies, confirms the general aspects of the predicted band structure but differs substantially in detail, finding an extremely elongated elliptical 2D pocket of ~ 5% of FBZ area and an effective mass of $1.9m_e$ (m_e is the free-electron mass). An unusual decrease of the Shubnikov–de Haas signal amplitude upon lowering the temperature has also been observed at high magnetic fields.[20] Most recently, measurements of anisotropic interlayer magnetoresistance[21,22] and anomalous Shubnikov–de Haas oscillations[23] have been reported and analyzed. The upper critical field of β''-$(ET)_2SF_5CH_2CF_2SO_3$ has been extracted via detailed specific-heat measurements, and the H-T phase diagram has been mapped out.[19,24] The Sommerfeld constant is larger than the band-structure prediction by a factor of ~ 3, and the estimated coupling constant ($\lambda \approx 1.1$) seems to suggest a phonon-mediated strong-coupling mechanism in this compound.[24] Taken together, the aforementioned experiments emphasize the important role of many-body effects in this material.

In general, the electronic spectra of low-dimensional organic metals deviate significantly from a conventional free-electron response. The origin of this deviation may vary for different samples and has been a subject of controversy. Whereas in quasi-1D organic conductors, the non-Drude response[25,26] may be attributed to Tomonaga-Luttinger liquid behavior of 1D interacting electronic systems, 2D ET-based organic conductors display a more complex optical response,[27] due to the involvement of a controversial infrared band often assigned to the interband transition resulting from 2D nature of the band structure.[28–30] At the same time, a number of experiments have demonstrated that electron cor-

relations in ET-based conductors play a significant role in their physical behaviors, putting many in the vicinity of a Mott metal-insulator transition.[31] Thus, strong correlation effects may be the origin of the unconventional optical properties in 2D organic solids. Consequently, the infrared band in the optical conductivity has been attributed to an effective Hubbard gap or an Abrikosov-Suhl resonance.[32,33] Further, there is some evidence that a FS (or quasiparticles) may not even exist in these "bad metal" systems at all.[34,35] Here, the "relevant resistivity scale" is on the order of $(h/e^2B)c$, where c is the interlayer spacing and B is a constant of order one.[32,34] In the spectroscopic response, optical conductivities of several β-phase superconductors show a transfer of spectral weight to low energy and development of a gap structure (or pseudogap) in the infrared with decreasing temperature.[27,36] The coherent Drude components cannot be estimated in these compounds due to either a broad overlap with a very strong pseudogap or an extremely narrow width of the Drude term. On the other hand, κ-type salts show the development of a Drude-like response at low temperatures accompanied by a broad absorption between 2000 and 3500 cm^{-1}.[30] Here, the appearance of the free-carrier response makes κ-$(ET)_2Cu(SCN)_2$ closer to a normal metal, although it still leaves the middle infrared structure as an anomaly. The similarity between the ET-based superconductors and high-temperature cuprate superconductors has also been noticed in various aspects and ascribed to the 2D nature and strong electron correlations in both systems.[32,37] This similarity is particularly striking for the underdoped cuprates where the pseudogap state is a dominant feature.[38]

Infrared vibrational features in conducting ET salts are usually superimposed upon the broad electronic background. It is well established that most of the observed phonon features are due to the totally symmetric A_g modes of intramolecular vibrations which couple strongly to the electronic excitations.[39–43] Therefore, vibronic features provide a window into both vibrational and electronic interactions in ET-based organic conductors. Previous infrared and Raman studies on various phases of ET conductors,[44–47] κ phase in particular,[30,48,49] have provided comprehensive assignments of intramolecular phonon modes. Normal-coordinate analysis has been performed,[46,47,50] and the results show good agreement with measurements. Isotope decoration studies have aided greatly in detailed mode assignments.

In order to provide an infrared and optical characterization of this type of superconductor and extract further information on the nature of the vibrational and electronic processes in the material, we have investigated the polarized infrared and optical response of β''-$(ET)_2SF_5CH_2CF_2SO_3$ as a function of temperature. We discuss our results in comparison with other ET-based superconductors as well as the copper oxide systems. Our overall goal is to understand the correlation between the crystal architecture and the physical properties in both normal and superconducting states.

II. EXPERIMENT

High-quality single crystals of β''-$(ET)_2SF_5CH_2CF_2SO_3$ ($1.2 \times 10 \times 0.3$ mm^3) were grown via electrochemical techniques in an H cell at Argonne National Laboratory.[8] The crystals are elongated

TABLE I. Assignments of vibrational features (in cm^{-1}) in the 10 K spectrum of β''-(ET)$_2$SF$_5$CH$_2$CF$_2$SO$_3$.

$\perp b$	$\| b$	Assignment [a]	Character
	2983 w	$\nu_{44}(b_{2u})$ or anion	CH stretching
2930 w [a]	2938 vw	$\nu_1(a_g)$	CH stretching
1452 vw	1451 vw	$\nu_2(a_g)$	C=C stretching
1406 vw	1414 vw	Anion multiplet	
1352 vw	1350 vw	$\nu_4(a_g)$ or Anion	C=C stretching
1300 vs	1200 vs	$\nu_3(a_g)$	C=C stretching
1297 w	1299 vw	$\nu_5(a_g)$ related	CH bending
1289 w	1275 w	$\nu_5(a_g)$ related	
1280 w		$\nu_5(a_g)$ related	
1269 w		$\nu_5(a_g)$ related	
1258 s	1257 m	Anion	CF stretching
1209 w	1211 vw	Anion?	CH bending
1183 m		$\nu_{38}(b_{2g})$ related	CH bending
1173 m		$\nu_{38}(b_{2g})$ related	
1138 vw		$\nu_{21}(b_{1g})$ related	CH bending
1126 w	1128 vw	$\nu_{21}(b_{1g})$ related	
1093 w	1096 vw	Anion	SO$_3$ stretching
993 w	990 m	Anion	SO$_3$ stretching
905 w		$\nu_7(a_g)$ or $\nu_{48}(b_{2u})$ or $\nu_{49}(b_{2u})$	C-C stretching, CH bending
881 s		$\nu_{60}(b_{3g})$ related	C-S stretching
875 s		$\nu_{60}(b_{3g})$ related	
852 s	852 w	Anion	SF$_5$ stretching
820 w	825 w	Anion	
799 w	795 vw	Anion	
657 w	661 vw	Anion	
622 m	629 w	Anion	
599 s	599 vw	Anion	
568 m		Anion	
551 m	549 vw	Anion	
522 m	522 vw	Anion	
455 vs	451 s	$\nu_{10}(a_g)$	C-S stretching
439 vs	438 s	$\nu_9(a_g)$	C-S stretching
318 m	322 m	$\nu_{11}(a_g)$	Ring deformation
240 m	248 m	Out-of-plane mode	

[a]vs is very strong, s is strong, m is medium, w is weak, and vw is very weak.
[b]References 44–49.

plates with the long axis of the crystal being the b axis and the large face containing the conducting ab plane. The high quality of the crystal samples was confirmed by the sharp superconducting transition at 5.2 K in the ac susceptibility.[51] For our measurements, two crystals were mounted to form a mosaic sample with size of 3×3 m^2.

Polarized infrared reflectance measurements were performed with a Bruker IFS 113V Fourier transform infrared spectrometer (35–5000 cm^{-1}), using a He-cooled bolometer detector in the far-infrared region (35–650 cm^{-1}). The spectra in the optical regime were collected on a Perkin-Elmer Lambda-900 spectrometer (4000–35 000 cm^{-1}), which is a grating instrument. Traditional room temperature detectors were employed over the middle and near-infrared (MIR, NIR), optical, and ultraviolet (UV) region. Standard polarizers were used to cover the aforementioned energy ranges. Temperature control was achieved with an open-flow APD

cryostat system. The temperature dependence of the infrared spectra was measured from 300 to 10 K. As the lowest temperature we can reach with this setup is $\sim$10 K, we probe the normal-state response of this sample here. Only room-temperature spectra were measured in the NIR/optical/UV range, providing a good extrapolation to the lower frequency temperature dependent data for the Kramers-Kronig analysis. An overcoat of Al was used to renormalize for the mosaic nature of the sample.

The wide frequency range of the measurement allows us to make a Kramers-Kronig analysis to obtain the optical constants of the material. These include the frequency-dependent conductivity $\sigma_1(\omega)$, the dielectric constant $\epsilon_1(\omega)$, and the effective mass $m^*(\omega)$.[52] The high-frequency extrapolation to the Kramers-Kronig phase shift integral was performed as $\omega^{-1.8}$. The low-frequency extrapolation was done with both metallic (Hagen-Rubens-type) and constant
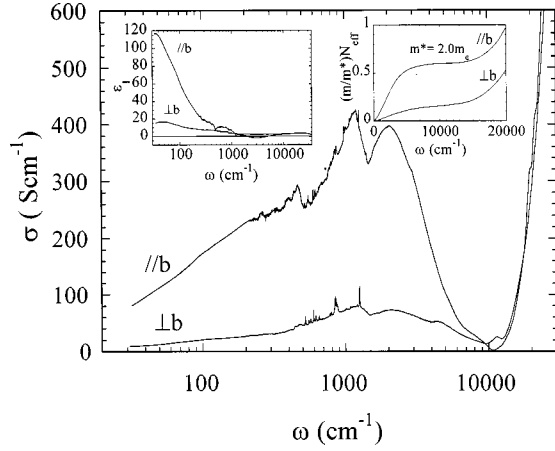
FIG. 2. Room-temperature frequency-dependent conductivity of β''-(ET)$_2$SF$_5$CH$_2$CF$_2$SO$_3$. Left inset: dielectric constant of β''-(ET)$_2$SF$_5$CH$_2$CF$_2$SO$_3$ as a function of frequency. Right inset: conductivity sum rule for β''-(ET)$_2$SF$_5$CH$_2$CF$_2$SO$_3$.

extrapolations;[52] little difference was obtained in the measurement regime.

III. RESULTS

A. Room temperature spectra

The 300 K reflectance of β''-(ET)$_2$SF$_5$CH$_2$CF$_2$SO$_3$ is shown in Fig. 1 in the two principle polarization directions. Overall, the response is similar to other known β''-type ET samples[53,54] and consistent with the β''-type crystal structure as well. The reflectance in the b direction (interstack) is significantly larger than that in the $\perp b$ direction ($\sim \| a$, i.e., ET stack), and shows a well-defined plasma edge. Nevertheless, this response is characteristic of a weak metal, certainly not that of a good conductor. On the other hand, reflectance in the $\perp b$ direction displays overdamped behavior with no clear plasma edge because $\tau \gg \omega_p$. The vast majority of the vibrational structure is observed perpendicular to b, where ET dimers are stacked in a face-to-face fashion. At the same time, vibrational bands are rather weak along b due to structural and screening effects. Our assignments for these features are given in Table I.

The 300 K frequency-dependent conductivity of β''-(ET)$_2$SF$_5$CH$_2$CF$_2$SO$_3$ is shown in Fig. 2. Optically, this material is fairly anisotropic, and the resemblance between the data in Fig. 2 and the response of several β-type conductors and superconductors [(ET)$_2$I$_3$, (ET)$_2$AuI$_2$, and β-(ET)$_2$I$_2$Br] is striking.[27,36] Compared to the SF$_5$CH$_2$CF$_2$SO$_3^-$ material, it is notable that the optical anisotropy of the β''-(ET)$_4$Fe(ox)$_3$H$_2$OC$_6$H$_5$CN superconductor is more severe,[10,55] suggesting that a range of optical anisotropies can give rise to the superconducting ground state in the β-packing motif. The anisotropy of κ-(ET)$_2$Cu(SCN)$_2$ is milder.[30] In contrast to the optical conductivity, the microwave conductivity of β''-(ET)$_2$SF$_5$CH$_2$CF$_2$SO$_3$ (measured from ESR) shows an anisotropy of $\sigma_b/\sigma_a \approx 1.4$.[14,15] Extrapolation of our optical conductivity to zero frequency provides an estimate of the dc conductivity, which is the same order of magnitude as the

300 K value (~ 6 Ω^{-1}cm^{-1}). A broad electronic band centered at ~ 2000 cm^{-1} is found for both $\| b$ and $\perp b$ polarizations, although it is clearly much stronger along b. The strong absorptions above $10\,000$ cm^{-1} are assigned as the intramolecular excitations.

The left-hand inset of Fig. 2 displays the 300 K frequency-dependent dielectric constant of β''-(ET)$_2$SF$_5$CH$_2$CF$_2$SO$_3$. Here, $\epsilon_1(\omega)$ is positive for both polarizations at low frequency, extrapolating to static values of ≈ 120 and 15 for $\| b$ and $\perp b$, respectively. There is strong dielectric contrast at low frequencies. The high-energy dielectric constant is ≈ 3 for both polarizations. From the zero crossing of ϵ_1, we estimate a screened plasma frequency of ≈ 4700 cm^{-1}. This corresponds to an unscreened ω_p ≈ 8100 cm^{-1} at 300 K, lower than that reported for I$_3^-$, I$_2$Br$^-$, and AuI$_2^-$ systems,[27,36] mainly due to the difference in $\epsilon_1(\infty)$ rather than the screened plasma frequency. The sum rule relates the oscillator strength to the effective mass and the effective number of carriers per formula unit participating in optical transitions (right-hand inset of Fig. 2). We estimate the effective electron mass by integrating the conductivity spectrum from 35 to 5000 cm^{-1} and assuming a carrier concentration resulting from 1 hole per dimer. We find $m_b^* \approx 2m_e$. Previous estimates from Shubnikov–de Haas oscillation measurements set $m^* \approx 1.9m_e$,[17] although direct comparison is not straightforward as different parts of the band are sampled.

B. Temperature dependence

The upper panels of Figs. 3 and 4 display the reflectance of β''-(ET)$_2$SF$_5$CH$_2$CF$_2$SO$_3$ at various temperatures for $\| b$ and $\perp b$ polarizations, respectively. In each direction, the middle infrared reflectance increases with decreasing temperature and seems to agree with the metallic dc conductivity, but the far-infrared response shows a flattening or a drop at lower temperatures, rather than an increase towards unity at low frequency. A similar response is observed in β-(ET)$_2$AuI$_2$ and β-(ET)$_2$I$_2$Br.[36] A close-up view of the low-energy data is given in the inset of each figure.

The frequency-dependent conductivity of β''-(ET)$_2$SF$_5$CH$_2$CF$_2$SO$_3$ as a function of temperature is shown in the lower panels of Figs. 3 and 4 for the $\| b$ and $\perp b$ polarizations, respectively. The electronic part of $\sigma_1(\omega)$ increases with decreasing temperature, particularly below 1200 cm^{-1}, and it drops in the far-infrared frequency range. Thus, the low-temperature spectra remain characteristic of a weak metal even down to 14 K, which is quite close to T_c. The spectral weight in the infrared is enhanced continuously with reduction of temperature. No Drude response develops in the spectra over the temperature and frequency range of our investigation. Note that the extrapolation of the low-frequency conductivity is in reasonable agreement with the dc values. Vibrational features are superimposed on this electronic background, as discussed below.

Figure 5 shows the detailed temperature dependence of the infrared vibrational spectrum polarized in the $\perp b$ direction. The strong peak at 1258 cm^{-1}, and several weaker ones in the pattern between 500 and 650 cm^{-1}, do not change significantly with temperature except for the usual narrowing. They are assigned as anion vibrations, as indicated in

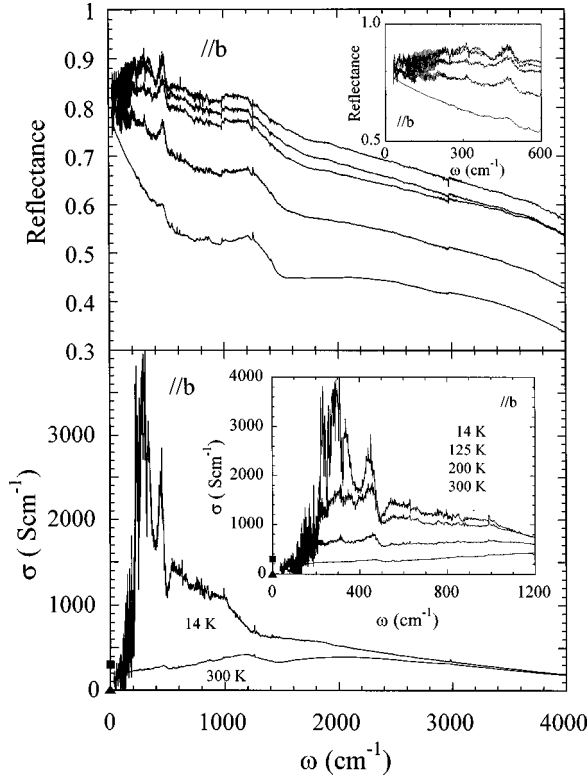FIG. 3. Upper panel: near normal reflectance of β''-(ET)$_2$SF$_5$CH$_2$CF$_2$SO$_3$ as a function of temperature along the b direction. Inset: closeup of the far-infrared reflectance. From top to bottom, temperatures are 14, 65, 125, 200, and 300 K. Lower panel: frequency-dependent conductivity of β''-(ET)$_2$SF$_5$CH$_2$CF$_2$SO$_3$ at 300 and 14 K in the b polarization. Inset: closeup of the low-frequency conductivity along b as a function of temperature. Note that in the lower panel, several temperatures have been omitted for clarity. dc conductivity data are indicated by triangle (300 K) and square (14 K).

FIG. 4. Upper panel: near normal reflectance of β''-(ET)$_2$SF$_5$CH$_2$CF$_2$SO$_3$ as a function of temperature in the $\perp b$ direction. Inset: closeup of the far-infrared reflectance. From top to bottom, temperatures are 14, 65, 125, 200, and 300 K. Lower panel: frequency-dependent conductivity of β''-(ET)$_2$SF$_5$CH$_2$CF$_2$SO$_3$ at 300 and 14 K in the $\perp b$ polarization. Inset: closeup of the low-frequency conductivity $\perp$ to b as a function of temperature. Note that in the lower panel, several temperatures have been omitted for clarity. dc conductivity data are indicated by triangle (300 K) and square (14 K).

Table I. The structures near 850 and 1095 cm^{-1}, which change with temperature, are also assigned as anion features. These assignments are in good agreement with the middle infrared spectrum of powdered Li-SF$_5$CH$_2$CF$_2$SO$_3$.[56] The anion modes appear mainly in the $\perp b$ direction. This is because the counterions are oriented along the ET stacks, and the strongest vibrational modes are polarized mainly along the length of the SF$_5$CH$_2$CF$_2$SO$_3^-$ anion; the electronic screening is lower in this direction as well. Apart from the counterion modes, the major infrared features are vibronically activated, as observed in other ET-based organic molecular conductors. In β''-$(ET)_2$SF$_5$CH$_2$CF$_2$SO$_3$, they are located mainly at 1350 (very broad), 880, and 439 cm^{-1}, as shown in Table I. Our symmetry assignments are generally consistent with those found in other ET salts.[44–46,49] Note that we have elected to assign the 881 and 875 cm^{-1} bands as $\nu_{60}(b_{3g})$,[49] rather than $\nu_7(a_g)$, but this is still a matter of disagreement in the literature. With decreasing temperature, the vibronic bands gradually increase in intensity and narrow significantly. No systematic splitting patterns were observed, although a few lines show weak multiplets at low temperature. The inset of Fig. 5 shows the C-H stretching mode pola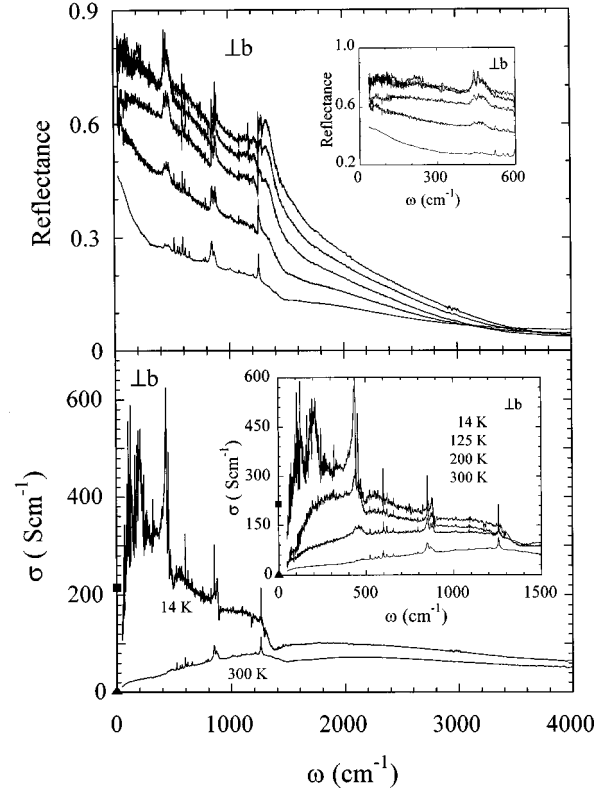rized $\parallel b$. This mode can be assigned either to C-H stretching of B_{2u} symmetry on the ET molecule or to the C-H stretching on the anion which is perpendicular to the long axis of the counterion. This band increases in intensity as the temperature drops.

IV. DISCUSSION

A. Electronic spectra

One of the most striking features of the optical conductivity in β''-(ET)$_2$SF$_5$CH$_2$CF$_2$SO$_3$ is the overall character of the spectra, which is weakly metallic at room temperature with a low-lying electronic band in the middle infrared. Such infrared localization is observed in a number of other β-type conductors and superconductors [(ET)$_2$I$_3$, (ET)$_2$AuI$_2$, and (ET)$_2$I$_2$Br],[27,36] as well as α_t-(ET)$_2$I$_3$,[57] which is similar to the β phase in structure. The various data sets on the aforementioned materials agree well in terms of position, polarization, and intensity of this feature. Although detailed temperature-dependent and far-infrared data are not available for the only other β''-type superconductor, (ET)$_4$[(H$_2$O)Fe(C$_2$O$_4$)$_3$]C$_6$H$_5$CN ($T_c=7$ K), the reflectance shows a quasi-one-dimensional character,[55] with a
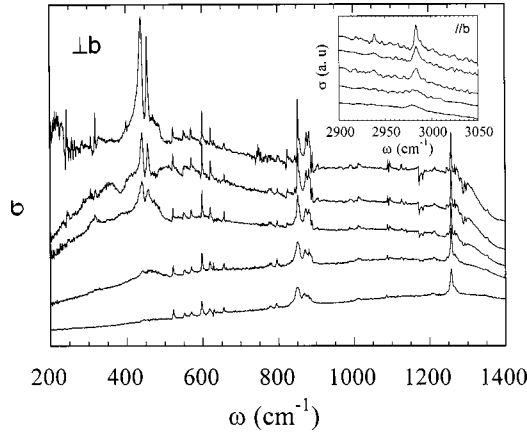
FIG. 5. Detailed frequency-dependent conductivity of β''-$(ET)_2SF_5CH_2CF_2SO_3$ as a function of temperature along the stacking direction ($\perp b$). Inset: frequency-dependent conductivity of β''-$(ET)_2SF_5CH_2CF_2SO_3$ in the C-H stretching regime along the b axis as a function of temperature. From top to bottom in the main figure and the inset, temperatures are 14, 65, 125, 200, and 300 K. Note that the curves are offset for clarity.

similar middle-infrared band in the conducting direction. Likely, measurement of the far infrared and a calculation of $\sigma_1(\omega)$ would reveal a corresponding low-energy electronic band. Electronic correlation as well as low carrier densities are believed to be the major mechanisms behind this localization phenomena.

Overall, β''-$(ET)_2SF_5CH_2CF_2SO_3$ maintains a similar localized response down to 14 K, which is just above T_c. The low-lying electronic band displays a significant enhancement and redshifting with decreasing temperature. The buildup of oscillator strength in the far-infrared may be related to increased interdimer interaction at low temperature, as predicted theoretically.[18] It is notable that the partial sum rule on $\sigma_1(\omega)$ is violated in β''-$(ET)_2SF_5CH_2CF_2SO_3$ as the temperature decreases. Sum rule violations can appear in strongly correlated systems, but the trend observed here is pronounced. Previous investigations of β-type molecular conductors show that the temperature dependence of oscillator strength is not straightforward. For instance, although the spectral weight is conserved fairly well in both polarizations for β-$(ET)_2I_2Br$ and β-$(ET)_2I_3$, in β-$(ET)_2AuI_2$, the spectral weight in the low-temperature phase is significantly larger than that in the high-temperature phase for each polarization ($\approx 1.25 : 1.0$ and $\approx 1.8 : 1.0$ for $\|$ and $\perp$ to the stacking direction, respectively).[27,36]

Most importantly, no distinct Drude component is found in the 14 K spectra of β''-$(ET)_2SF_5CH_2CF_2SO_3$ within noise level and frequency range of our investigation. This is unlike a conventional metal, where a significant free-carrier contribution is expected due to highly mobile carriers. Based on the moderate value of σ_{dc} just above T_c (~ 300 Ω^{-1} cm^{-1}), it is reasonable not to see a strong Drude peak in the $SF_5CH_2CF_2SO_3^-$ compound. The small Fermi surface and estimates of the carrier concentration from transport measurements are also in line with the lack of a free-carrier response in the optical spectra. However, the observation of magnetoresistance oscillations at low temperature suggests that the sample is very clean, as the Dingle temperature is 0.5

K and the scattering rate is small.[17] A possible resolution may arise from the fact that in a strongly correlated metal near a metal $\rightarrow$ insulator transition, one expects to observe very little Drude weight in the optical response. However, $m^* \sim 2$ (optical measurements) or 1.9 (magnetoresistance measurements), leading to an impass. It is likely that any Drude response in β''-$(ET)_2SF_5CH_2CF_2SO_3$ is fairly weak and/or very narrow. Microwave dielectric measurements would be useful to compliment the far-infrared data presented here.

The very narrow or absent free-carrier response in β''-$(ET)_2SF_5CH_2CF_2SO_3$ extends to the aforementioned β-phase superconductors. It is especially pronounced in β-$(ET)_2AuI_2$. Previously, the non-Drude behavior in the β materials was attributed to strong electron-electron and electron-phonon interactions.[27,36] This trend is in contrast to the κ-$(ET)_2Cu(SCN)_2$ prototype, where a Drude contribution in the optical spectra is observed well above T_c.[30] A low-frequency free-carrier response is also found in α-$(ET)_2(NH_4)Hg(NCS)_2$,[58] where the overlap is strong and the band structure looks like that of the κ phase. These results suggest that ET-based solids in the β-packing motif may approach the superconducting transition quite differently than the more 2D κ-phase counterparts.

For underdoped copper oxide superconductors, the normal-state in-plane spectra are composed of a coherent Drude-like component and a broad mid-infrared band.[59] This two-component response is characteristic of many other low-dimensional correlated systems.[60] Below T_c, the Drude part condense into a superfluid whereas the mid-infrared band remains. In some high-temperature superconductors, a far-infrared peak, rather than a Drude component, is also observed and may be attributable to the disorder-induced localization.[61]

It is an ongoing challenge to understand the origin of the low-energy electronic band in β''-$(ET)_2SF_5CH_2CF_2SO_3$. This sort of structure is found in all of the ET-based organic solids and several models have been proposed to account for its presence.[28,29,32,33,62] Approaches based upon the Hubbard model have attracted a great deal of attention recently. In one application, the Hubbard model has been used to study the optical conductivity of highly correlated electron systems in a dynamic mean-field approximation,[63] which becomes exact for either the infinite lattice connectivity or large spatial dimensionality. For metals in close proximity to the Mott metal-insulator transition, the theory predicts that the optical conductivity shows the development of a Drude peak, a resonance at an energy U due to the transitions between upper and lower Hubbard bands, and an enhancement of spectral weight below a critical temperature.[64]

The optical conductivity of κ-$(ET)_2Cu(SCN)_2$ has been analyzed within this framework,[32,33] providing an estimate of U_{eff} from the experimental data. Here, U_{eff} is the Coulomb repulsion between two carriers on the same ET dimer. This theory seems to work quite well for the κ-type superconductors near the Mott transition on the metallic side. On the other hand, for β-type superconductors, the optical conductivity cannot be straightforwardly interpreted by this theory due to the absence of a Drude (free carrier) response in the low-temperature spectra. Further, if we assign the infrared charge-transfer structure seen in the β- and β''-type salts to transitions between upper and lower Hubbard bands, the fea-

ture is stronger and lower in energy compared with that in the κ-phase superconductors. A possible resolution of this discrepancy might lie with different Hubbard parameters in β-phase compounds compared with the κ salts as well as the weak dimerization in β''-$(ET)_2SF_5CH_2CF_2SO_3$.

To summarize, the β and β'' family of ET-based salts presents a consistent and challenging set of questions regarding the electronic structure which deserve fresh study, particularly from a theoretical point of view. Specifically, the very narrow or absent Drude response in the spectra at low temperature, the assignment of the infrared band, and the temperature dependence of this low-lying excitation (which causes the conductivity sum rule to be violated so strongly in the $SF_5CH_2CF_2SO_3^-$ compound) present important challenges in these systems.

B. Vibrational features

According to various electron-phonon coupling theories, vibronic band intensities are directly related to the oscillator strength of the nearby electronic band and the lattice distortion caused by the coupling.[39–43] Thus, vibronic features are well known to provide a microscopic probe of the interactions in organic solids, with mode intensities relating directly to the square of the order parameter of the lattice distortion. In β''-$(ET)_2SF_5CH_2CF_2SO_3$, the high-temperature coupling-allowed features are weak in $\perp b$ polarization; even the three strongest vibronic modes (1350, 890, and 439 cm^{-1}) are barely visible. Upon lowering the temperature, these features increase significantly in intensity (Fig. 5). However, we cannot conclude that the increasing strength of the vibronic bands is solely due to enhancement and redshifting of the electronic band. In fact, the electronic conductivity in the far-infrared seems to saturate below 60 K, whereas intensities of several vibronic bands increase continuously. The lattice may continue to dimerize at low temperature, which may be responsible for the changing of vibrational features.

A few low-energy vibrational features are also observed to change upon approach to T_c in β''-$(ET)_2SF_5CH_2CF_2SO_3$. In contrast to the aforementioned temperature dependence of other modes, the far-infrared structures at 318 $[\nu_{11}(a_g)]$ and 240 cm^{-1} (an out-of-plane mode according to Ref. 49) are very weak down to 60 K, but they show up clearly in the 14 K spectrum (Fig. 5). This may indicate the involvement of these low-energy vibrational modes in driving the superconducting transition in β''-$(ET)_2SF_5CH_2CF_2SO_3$. Alternatively, these vibrational changes may be indicative of a weak structural modification at low temperature.

The $\nu_3(a_g)$ vibrational mode (mainly related to central C=C stretching in the ET molecule) is very broad and damped in β''-$(ET)_2SF_5CH_2CF_2SO_3$ in the $\perp b$ direction. A similarly broad ν_3 band has been observed in α-$(ET)_2(NH_4)Hg(NCS)_4$,[58] although in other β and κ phase ET salts, this mode is much narrower. This difference may be related to the degree of dimerization. The band shape of $\nu_3(a_g)$ in β''-$(ET)_2SF_5CH_2CF_2SO_3$ is also derivativelike, indicating a strong interaction and overlap with the low-energy electronic background. While this unusual line shape is visible at 300 K, it is seen more clearly at low temperatures and is characteristic of a Fano resonance.[65]
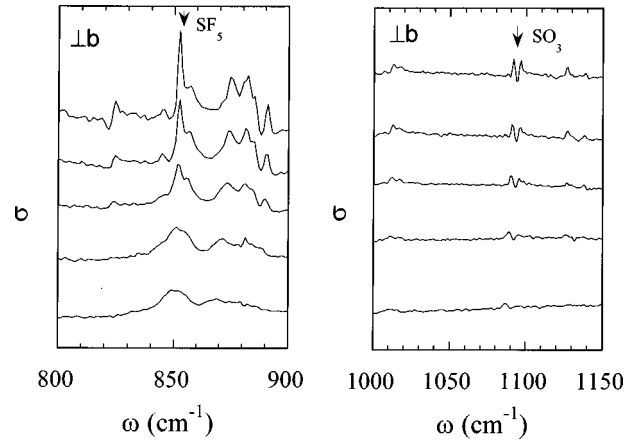

FIG. 6. Detailed frequency-dependent conductivity of β''-$(ET)_2SF_5CH_2CF_2SO_3$ as a function of temperature along the $\perp b$ direction in the SF_5 and SO_3 stretching vibrational region of the anion. From top to bottom in the two panels, temperatures are 14, 65, 125, 200, and 300 K. Note that the curves are offset for clarity.

Because intermolecular hydrogen bonding is anticipated between the ethylene endgroups of the ET molecule and the SF_5 and SO_3 endgroups of the counterion, the vibrational features of anion, especially the modes associated with the SF_5 and SO_3 groups, may provide information about this interaction. Based upon existing reference spectra for the SO_3 and SF_5 functional groups,[66,67] we assign the weak band at 1093 cm^{-1}, and a strong one at 852 cm^{-1} to the stretching vibrations of the SO_3 and SF_5 groups in the anion, respectively. Closeup views of these modes are presented in Fig. 6. The SO_3 stretching mode (1093 cm^{-1}) displays doublet splitting and a systematic increase in intensity towards low temperatures. The SF_5 stretching mode (852 cm^{-1}) is rather broad at high temperature, probably due to the significant hydrogen bonding formed between SF_5 and the ethylene end unit of the ET molecules. However, at low temperature, doublet structure is observed, combined with a distinct linewidth narrowing. Taken together, the thermal evolution of these phonon bands may indicate a weak structural change with temperature, which probably modifies the hydrogen bonding between the ET building block molecules and anions. This weak reorganization of interactions within the anion pocket may ultimately aid in stabilizing the superconducting ground state. The driving force of this change, and correlation with the unusual electronic band if any, are interesting issues and worth exploring in the future. Microscopic probes of chemical structure effects on H bonding in the anion pocket should be most effective. In β''-$(ET)_4[(H_2O)Fe(C_2O_4)_3]C_6H_5CN$, the important interaction seems to be with the intercolated water molecules,[10,11,55] rather than between the ET building block molecule and the anion.

V. CONCLUSION

We have investigated the polarized infrared and optical reflectance of β''-$(ET)_2SF_5CH_2CF_2SO_3$ as a function of temperature. This fully organic superconductor displays weak metallic behavior over the full temperature range of

our investigation. Even a few degrees above T_c, it does not exhibit a Drude response within our resolution. Instead, far-infrared localization is observed. It is notable that other β and β'' superconductors display similar non-Drude behavior before moving into the superconducting phase. Vibronic features increase in intensity with decreasing temperature in the infrared, as expected. Structural measurements indicate that distances within the anion pocket are reasonable for the intermolecular hydrogen bonding to occur, and the temperature dependence of key anion vibrational modes suggests changes in this coupling, which is related to a possible structural modification at low temperature. Our ongoing investigations with other $SF_5RSO_3^-$ complexes should further clarify this matter.

[1] T. Ishiguro and K. Yamaji, *Organic Superconductors*, 2nd. ed. (Springer-Verlag, Berlin, 1997).

[2] J. Wosnitza, *Fermi Surfaces of Low Dimensional Organic Metals and Superconductors* (Springer-Verlag, Berlin, 1996).

[3] J.M. Williams, J.R. Ferraro, K.D. Carlson, U. Geiser, H.H. Wang, A.M. Kini, and M.H. Whangbo, *Organic Superconductors* (Prentice-Hall, Englewood Cliffs, NJ, 1992).

[4] A.M. Kini, U. Geiser, H.H. Wang, K.D. Carlson, J.M. Williams, W.K. Kwok, K.G. Vandervoort, J.E. Thompson, D.L. Stupka, D. Jung, and M.H. Whangbo, Inorg. Chem. **29**, 2555 (1990).

[5] J.M. William, A.M. Kini, H.H. Wang, K.D. Carlson, U. Geiser, L.K. Montgomery, G.J. Pyrka, D.M. Watkins, J.M. Kommers, S.J. Boryschuk, A.V. Strieby Crouch, W.K. Kwok, J.E. Schirber, D.L. Overmyer, D. Jung, and M.H. Whangbo, Inorg. Chem. **29**, 3262 (1990).

[6] J.A. Schlueter, J.M. Williams, U. Geiser, J.D. Dudek, M.E. Kelly, S.A. Sirchio, K.D. Carlson, D. Naumann, T. Roy, and C.F. Campana, Adv. Mater. **7**, 634 (1995).

[7] J.A. Schlueter, K.D. Carlson, U. Geiser, H.H. Wang, J.M. Williams, W.-K. Kwok, J.A. Fendrich, U. Welp, P.M. Keane, J.D. Dudek, A.S. Komosa, D. Naumann, T. Roy, J.E. Schirber, W.R. Bayless, and B. Dodrill, Physica C **233**, 379 (1994).

[8] U. Geiser, J.A. Schlueter, H.H. Wang, A.M. Kini, J.M. Williams, P.P. Sche, J.I. Zakowicz, M.L. VanZile, and J.D. Dudek, J. Am. Chem. Soc. **118**, 9996 (1996).

[9] H.H. Wang, M.L. VanZile, J.A. Schlueter, U. Geiser, A.M. Kini, P.P. Sche, H.J. Koo, M.H. Whangbo, P.G. Nixon, R.W. Winter, and G.L. Gard, Synth. Met. (to be published).

[10] M. Kurmoo, A.W. Graham, P. Day, S.J. Coles, M.B. Hursthouse, J.L. Caulfield, J. Singleton, F.L. Pratt, W. Hayes, L. Ducasse, and P. Guionneau, J. Am. Chem. Soc. **117**, 12 209 (1995).

[11] L. Martin, S.S. Turner, P. Day, F.E. Mobbs, and E.J.L. McInnes, J. Chem. Soc. Chem. Commun. **1997**, 1367.

[12] J.A. Schlueter (private communication).

[13] S. Sadewasser, C. Looney, J.S. Schilling, J.A. Schlueter, J.M. Williams, P.G. Nixon, R.W. Winter, and G.L. Gard, Solid State Commun. **104**, 571 (1997).

[14] H.H. Wang, M.L. VanZile, U. Geiser, J.A. Schlueter, J.M. Williams, A.M. Kini, P.P. Sche, P.G. Nixon, R.W. Winter, G.L. Gard, D. Naumann, and T. Roy, Synth. Met. **85**, 1533 (1997).

[15] H.H. Wang, M.L. VanZile, J.A. Schlueter, U. Geiser, A.M. Kini, P.P. Sche, H.J. Koo, M.H. Whangbo, P.G. Nixon, R.W. Winter, and G.L. Gard (unpublished).

[16] T. Mori, F. Sakai, G. Saito, and H. Inokuchi, Chem. Lett. **1986**, 1037.

[17] D. Beckmann, S. Wanka, J. Wosnitza, J.A. Schlueter, J.M. Williams, P.G. Nixon, R.W. Winter, G.L. Gard, J. Ren, and M.-H. Whangbo, Eur. Phys. J. B **1**, 295 (1998).

[18] J.A. Schlueter, U. Geiser, H.H. Wang, M.L. VanZile, J.M. Williams, H.J. Koo, M.H. Whangbo, P.G. Nixon, R.W. Winter, and G.L. Gard (unpublished).

[19] J. Wosnitza, G. Goll, D. Beckmann, S. Wanka, J.A. Schlueter, J.M. Williams, P.G. Nixon, R.W. Winter, and G.L. Gard, Physica B **246-247**, 104 (1998).

[20] J. Wosnitza, S. Wanka, J.S. Qualls, J.S. Brooks, C.H. Mielke, N. Harrison, J.A. Schlueter, J.M. Williams, P.G. Nixon, R.W. Winter, and G.L. Gard, Synth. Met. (to be published).

[21] X. Su, F. Zuo, J.A. Schlueter, J.M. Williams, P.G. Nixon, R.W. Winter, and G.L. Gard, Phys. Rev. B **59**, 4376 (1999).

[22] X. Su, F. Zuo, J.A. Schlueter, and J.M. Williams, Phys. Rev. B **59**, 4376 (1999).

[23] F. Zuo, X. Su, P. Zhang, J.S. Brooks, J. Wosnitza, J.A. Schlueter, J.M. Williams, P.G. Nixon, R.W. Winter, and G.L. Gard (unpublished).

[24] S. Wanka, J. Hagel, D. Beckmann, J. Wosnitza, J.A. Schlueter, J.M. Williams, P.G. Nixon, R.W. Winter, and G.L. Gard, Phys. Rev. B **57**, 3084 (1998).

[25] N. Cao, T. Timusk, and K. Bechgaard, J. Phys. I **6**, 1719 (1996).

[26] M. Dressel, A. Schwartz, G. Grüner, and L. Degiorgi, Phys. Rev. Lett. **77**, 398 (1996).

[27] C.S. Jacobsen, J.M. Williams, and H.H. Wang, Solid State Commun. **54**, 937 (1985).

[28] H. Tajima, K. Yakushi, H. Kuroda, and G. Saito, Solid State Commun. **56**, 159 (1985).

[29] A. Ugawa, G. Ojima, K. Yakushi, and H. Kuroda, Phys. Rev. B **38**, 5122 (1988).

[30] K. Kornelsen, J.E. Eldridge, H.H. Wang, and J.M. Williams, Phys. Rev. B **44**, 5235 (1991).

[31] K. Kanoda, Physica C **282-287**, 299 (1997).

[32] R.H. McKenzie, J. Phys.: Condens. Matter (to be published).

[33] B.R. Bulka, Mol. Phys. Rep. (to be published).

[34] V.J. Emery and S.A. Kivelson, Phys. Rev. Lett. **74**, 3253 (1995).

[35] R. Liu, H. Ding, J.C. Campuzano, H.H. Wang, J.M. Williams, and K.D. Carlson, Phys. Rev. B **51**, 13 000 (1995).

[36] C.S. Jacobsen, D.B. Tanner, J.M. Williams, U. Geiser, and H.H. Wang, Phys. Rev. B **35**, 9605 (1987).

[37] R.H. McKenzie, Science **278**, 820 (1997).

[38] C.C. Homes, T. Timusk, R. Liang, D.A. Bonn, and W.N. Hardy, Phys. Rev. Lett. **71**, 1645 (1993).

[39] M.J. Rice, Phys. Rev. Lett. **37**, 36 (1976).

[40] M.J. Rice, Solid State Commun. **31**, 91 (1979).

[41] M.J. Rice, V.M. Yartsev, and C.S. Jacobsen, Phys. Rev. B **21**, 3437 (1980).

[42] R. Bozio and C. Pecile, *Spectroscopy of Advanced Materials*, edited by R.J.H. Clark and R.E. Hester (Wiley, Chichester, 1991), p. 1.

[43] V.M. Yartsev and A. Graja, Int. J. Mod. Phys. B **12**, 1643 (1998).

[44] M. Meneghetti, R. Bozio, and C. Pecile, J. Phys. (Paris) **47** (8), 1377 (1986).

[45] T. Sugano, H. Hayashi, M. Kinoshita, and K. Nishikida, Phys. Rev. B **39**, 11 387 (1989).

[46] M.E. Kozlov, K.I. Pokhodnia, and A.A. Yurchenko, Spectrochim. Acta A **43A** (3), 323 (1987).

[47] M.E. Kozlov, K.I. Pokhodnia, and A.A. Yurchenko, Spectrochim. Acta A **45A** (4), 437 (1989).

[48] J.E. Eldridge, Y. Xie, H.H. Wang, J.M. Williams, A.M. Kini, and J.A. Schlueter, Spectrochim. Acta A **52A**, 45 (1996).

[49] J.E. Eldridge, Y. Xie, Y. Lin, C.C Homes, H.H. Wang, J.M. Williams, A.M. Kini, and J.A. Schlueter, Spectrochim. Acta A **53A**, 565 (1997).

[50] J.E. Eldridge, C.C. Homes, J.M. Williams, A.N. Kini, H.H. Wang, Spectrochim. Acta A **51A** (6), 947 (1995).

[51] ΔT_c (10–90 %) = 0.8 K.

[52] F. Wooten, *Optical Properties of Solids* (Academic, New York, 1972).

[53] A. Ugawa, Y. Okawa, K. Yakushi, H. Kuroda, A. Kawamoto, J. Tanaka, M. Tanaka, Y. Nogami, S. Kagoshima, K. Murata, and T. Ishiguro, Synth. Met. **27**, A407 (1988).

[54] F.L. Pratt, W. Hayes, M. Kurmoo, and P. Day, Synth. Met. **27**, A439 (1988).

[55] S.J. Blundell, A.A. House, J. Singleton, M. Kurmoo, F.L. Pratt, P.A. Pattenden, W. Hayes, A.W. Graham, P. Day, and J.A.A.J. Perenboom, Synth. Met. **85**, 1569 (1997).

[56] G.L. Gard (private communication).

[57] V. Železný, J. Petzelt, R. Swietlik, B.P. Gorshunov, A.A. Volkov, G.V. Kozlov, D. Schweitzer, and H.J. Keller, J. Phys. (Paris) **51**, 869 (1990).

[58] M. Dressel, J.E. Eldridge, H.H. Wang, U. Geiser, and J.M. Williams, Synth. Met. **52**, 201 (1992).

[59] D.B. Tanner and T. Timusk, in *Physical Properties of High Temperature Superconductors III*, edited by D.M. Ginsberg (World Scientific, Singapore, 1992), p. 363.

[60] V. Vescoli, L. Degiorgi, H. Berger, and L. Forró, Phys. Rev. Lett. **81**, 453 (1998).

[61] T. Timusk, A.V. Puchkov, D.A. Bosov, and T. Startseva, J. Phys. Chem. Solids **59**, 1953 (1998).

[62] V.M. Yartsev, O.O. Drozdova, V.N. Semkin, and R.M. Vlasova, J. Phys. I **6**, 1673 (1996).

[63] A. Georges, G. Kotliar, W. Krauth, and M.J. Rozenberg, Rev. Mod. Phys. **68**, 13 (1996).

[64] M.J. Rozenberg, G. Kotliar, and H. Kajueter, Phys. Rev. B **54**, 8452 (1996).

[65] V. Fano, Phys. Rev. **124**, 1866 (1961).

[66] J.C. Evans and H.J. Bernstein, Can. J. Chem. **33**, 1270 (1955).

[67] D.F. Eggers, H.E. Wright, and D.W. Robinson, J. Chem. Phys. **35**, 1045 (1961).